

Polyelectrolyte-Mediated Bridging Interactions

RUDI PODGORNİK

Laboratory of Physical and Structural Biology, NICHD, Bld. 9, Rm. 1E116, National Institutes of Health, Bethesda, Maryland 20892-0924

Department of Physics, University of Ljubljana, Jadranska 19, 1000 Ljubljana, Slovenia

Department of Theoretical Physics, J. Stefan Institute, Jamova 39, SI-1000 Ljubljana, Slovenia

Received 10 November 2003; revised 12 January 2004; accepted 1 March 2004

DOI: 10.1002/polb.20205

Published online in Wiley InterScience (www.interscience.wiley.com).

ABSTRACT: Polyelectrolyte chains confined by macroions bearing electrostatic charges of opposite sign can mediate an effective attraction between the macroions. This polyelectrolyte-mediated attraction is usually referred to as the bridging interaction. I review the theories of polyelectrolyte-mediated interactions based on analytic mean-field and variational approaches. I will describe the origin and the salient properties of this interaction in the context of planar and point macroions with special emphasis on the connection between the polymer chain conformations and the ensuing polymer mediated interactions. © 2004 Wiley Periodicals, Inc. *J Polym Sci Part B: Polym Phys* 42: 3539–3556, 2004

Keywords: bridging interactions; polyelectrolyte chains

INTRODUCTION

Ubiquitous in colloidal systems and soft matter in general,^{1,2} charged polymers play a fundamental role in determining the interactions between as well as stability and structure of various (macro)-molecular assemblies. Statistical properties of charged polymers set them quite apart from the noncharged polymers.³ Their effect on colloidal interactions has been studied and exploited in various technological contexts ranging from the paper industry to the pharmaceutical industry.⁴ It seems, however, that their most basic role is played in the biological context. They are an essential and fundamental component of the cellular environment, and make their mark in its every structural and functional aspect.⁵ It is thus no

surprise that the behavior of charged polymer chains in biological context has been one of the major foci of soft matter research for quite a few years now.⁶

In charged colloidal system the interactions are usually subsumed under the heading of the DLVO theory.⁷ Within this framework the electromagnetic interactions between macroscopic bodies are broken into two disjoint contributions. First there is a contribution that has its origin in the creation of double layers in the bathing solution close to the charged surfaces.⁸ Their existence is due to the interplay of entropic effects, that favor homogeneous distribution of mobile charges, and electrostatic attraction between the charges on the surfaces and their counterions in the aqueous environment.⁹ This contribution to the total force between the surfaces is repulsive, if the surfaces bear charges of the same sign. The second contribution is usually attractive, irrespective of the charges on the surfaces; its origin is in the fluctuations (thermodynamic as well as

Correspondence to: R. Podgornik (E-mail: rudi@helix.nih.gov)

Journal of Polymer Science: Part B: Polymer Physics, Vol. 42, 3539–3556 (2004)
© 2004 Wiley Periodicals, Inc.

quantum mechanical) of the local electromagnetic fields in the component dielectric media. It is usually referred to as the van der Waals-Lifshitz interaction.¹⁰ In general, however, the two contributions are not additive or even separable.⁶

The addition of polyelectrolytes to the bathing solution demands a thorough generalization of the DLVO theory, especially its electrostatic part, that has to take into account the connectivity between charged segments along the polymer chain. This connectivity can often lead to a very peculiar interaction, where long charged polymers can mediate interactions between macroions of opposite charge.¹¹ The term *bridging interactions* is usually applied to this situation where a single chain can adsorb to different, two or more, macroions, and via its connectivity mediate attractive interactions between them. These interactions have been studied intensively both experimentally as well as theoretically. Surface force apparatus and atomic force microscopy¹² have provided direct data on the separation dependence of the bridging interaction between macroscopic surfaces with polyelectrolyte chains either grafted or in chemical equilibrium with a bulk solution. Theoretical work has added a clear mesoscopic picture for the bridging interaction between macroscopic surfaces and elucidated the effects of salt and nonelectrostatic excluded volume on the strength and range of this interaction.^{13–18} Because it is based on sometimes severe model or formal restrictions there is no single theoretical approach that is able to account for all experimentally observed details or is able to explore in comparable details all the regions of the parameter phase space.¹¹ Different approaches address different regions of the parameter space.

The problem of polyelectrolyte chains in the bulk, worked out at different levels of approximations,^{19,20} is reasonably well understood. On the other side, the case of a confined (neutral) polymers is also well understood, and the forces between confining surfaces have been studied at various levels of approximation.²¹ The two were first brought together, that is, charged interfaces with charged polymers, in the seminal work of Muthukumar.²² A further step was taken when the mean-field theory was applied to the problem of polyelectrolyte mediated interactions, starting from the work of van Opheusden.²³ Due to the connectivity of the polyelectrolyte chain the results of these model calculations based either on continuum¹⁴ or lattice-type²⁴ mean-field theories bear almost no resemblance to the case of con-

finied unconnected ions. A self-consistent field theory, akin to the usual Poisson-Boltzmann theory of electrostatic interactions in colloidal systems, has been proposed for confined polyelectrolytes and applied successfully to the problem of polyelectrolyte mediated interactions between charged surfaces.¹³ This approach has been later properly generalized to include also the effect of steric interactions between polymer segments on adsorption and polyelectrolyte mediated interaction.^{17,18} For small macroions with free¹⁶ or grafted²⁵ polyelectrolyte chains a different approach was found to be more convenient, based on a harmonic variational *ansatz*. It allows for an elegant and straightforward evaluation of the polyelectrolyte mediated interactions in the geometry where self-consistent field theory would be more difficult to solve.

In this short review of the problem of polyelectrolyte mediated interactions I will try to remain as close to the Poisson-Boltzmann (PB) approach to a confined electrolyte as possible. For planar surfaces with intervening polyelectrolytes I will describe a straightforward generalization of the Poisson-Boltzmann theory where the statistical averages over the polymeric degrees of freedom will be included in a self-consistent manner and will lead to pronounced polyelectrolyte-mediated bridging. In the opposite limit of small macroions with intervening oppositely charged polyelectrolyte chains I will review a different approach based on a harmonic variational, two particle (two macroions) theory of the bridging interaction. Again, the coupling between polyelectrolyte conformation and electrostatics will lead to pronounced bridging interactions with similar properties as in the planar case. I will estimate the salient features of the polyelectrolyte mediated interactions in both cases and indicate the regions of the parameter space where they might dominate the interaction. I will not specifically review the simulation work pertaining to the bridging interaction as well as the many experimental studies that are in one way or another relevant for the proper understanding of the different facets of the bridging effect.

PLANAR INTERFACES—SELF-CONSISTENT FIELD THEORY

The Model and Its Hamiltonian

The planar case is schematically represented on Figure 1. Polyelectrolyte chains and salt ions are

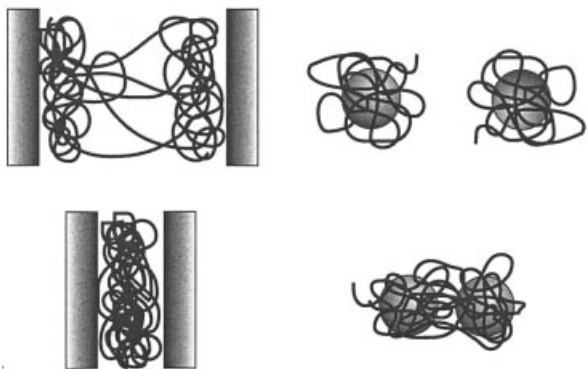


Figure 1. Schematics of the model for planar and point macroions. In the first case, the confinement of the chain at small intersurface separations gives rise to repulsive interactions. At larger spacings the chain assumes bridging conformations, partly adsorbed to one surface, partly to the other one, with segments of the chain spanning the region in between, conferring intersurface attractions. With small (ideally point) macroions the chains are bound to both of them at small separations, thus creating bridging configurations and conferring attractive interactions. At larger separations because of their finite length, the chains remain bound each to its own macroion, renormalizing its charge in a Debye-Hückel like repulsion.

confined between two oppositely charged surfaces of surface charge density σ (presumed negative) separated by $2a$, that are impenetrable to all mobile charges. The uni-uni valent electrolyte is described in the frame of the primitive model with ionic charge e_0 , dielectric constant ϵ and activity z_0 . For the level of subsequent approximations the hard-core radius is not important, so is the possible grafting of the chain. The effects of the latter would only show for short chains or if the grafting density would be high enough to create polyelectrolyte brushes.¹¹ Both these possibilities will not be addressed in what follows.

The polyelectrolyte chains are described in the frame of a continuum model as freely jointed links of charge τ per bead of Kuhn's length ℓ , with a total contour length equal to $N\ell$. The total number of polymer chains is \mathcal{N} . All electrostatic interactions are mediated by the Coulomb kernel of the form

$$u(\mathbf{r}, \mathbf{r}') = \frac{ee'}{4\pi\epsilon\epsilon_0|\mathbf{r} - \mathbf{r}'|}, \quad (1)$$

where e, e' refer to the charges located at \mathbf{r}, \mathbf{r}' . In what follows we will ignore the possibility of sta-

tistically distributed charges along the chain²⁶ and will assume them to be fixed and uniform. The configurational part of the Hamiltonian for this model system can be written as

$$\beta\mathcal{H}[\mathbf{r}_i] = \frac{3}{2\ell^2} \sum_{\alpha} \int_0^{N_{\alpha}} \left(\frac{d\mathbf{r}^{\alpha}(n)}{dn} \right)^2 dn + \frac{1}{2} \beta \sum_{i,j} u(\mathbf{r}_i, \mathbf{r}_j) - \frac{1}{2} \beta \sum_k N_k u(\mathbf{r}_k, \mathbf{r}_k) + \beta \sum_i e_i \phi_e(\mathbf{r}_i). \quad (2)$$

In the above equation $\mathbf{r}^{\alpha}(n)$ stands for the continuous coordinate of the n th bead along the α th polymeric chain, index i, j , and k run over all polymer beads of all the chains, all mobile salt anions and cations and $\beta = (kT)^{-1}$ is the inverse thermal energy. The first term corresponds to the chain connectivity, while the third term merely removes the self-energy terms ($i = j$) from the Hamiltonian. $\phi_e(\mathbf{r})$ is the external electrostatic potential due to the charges on the surfaces. In this form of the Hamiltonian the possibility of discrete surface charges as well as the presence of dielectric discontinuities was disregarded.

The Partition Function

In what follows we will closely follow the analysis of ref. 13. The partition function of the system characterized by the configurational Hamiltonian \mathcal{H} acknowledges the fact that the ions are allowed to exchange with the bulk reservoir as the separation between the surfaces varies. As for the polymeric chains, we assume that they are not in equilibrium with the bulk phase because the transverse diffusion rate of a polymer trapped between two surfaces is small, and the overall situation is one of restricted equilibrium. The appropriate partition function is therefore

$$\Xi = \prod_{\alpha} \prod_{s=a,c} \sum_{N_s=0}^{\infty} \frac{\zeta^{N_s}}{N_s!} \int_{[\mathbf{r}^{\alpha}, \mathbf{r}]} e^{-\beta\mathcal{H}} \mathcal{D}\mathbf{r}^{\alpha}(n) \mathcal{D}^{N_s}\mathbf{r} \quad (3)$$

where a, c stand for anions and cations, α is the index of polymeric chains, ζ is the renormalized value of the absolute activity and $\zeta = z_0 e^{(1/2)\beta e_0^2 u(\mathbf{r}, \mathbf{r})}$. The integration measures in the above equation are defined as: $\mathcal{D}\mathbf{r}^{\alpha}(n) = d^3\mathbf{r}^{\alpha}(1) d^3\mathbf{r}^{\alpha}(2) \dots d^3\mathbf{r}^{\alpha}(N_{\alpha})$ and $\mathcal{D}^{N_s}\mathbf{r} = d^3\mathbf{r}(1) d^3\mathbf{r}(2) \dots d^3\mathbf{r}(N_s)$ where $\mathbf{r}(N_s)$ is the position vector of the N_s -th anion or cation ($s = a, c$) respectively.

Introducing now the Hubbard-Stratonovich transformation permits us to write the pair interactions in an effective one-particle form, so that we can perform the summations in eq 3 explicitly remaining, apart from an irrelevant multiplicative factor, with the following compact form of the partition function²⁷

$$\Xi = \prod_{\alpha} \iint \langle G_{\phi}(\mathbf{r}^{\alpha}, \mathbf{r}'^{\alpha}; N^{\alpha}) d^3\mathbf{r}^{\alpha} d^3\mathbf{r}'^{\alpha} \rangle_{\phi}. \quad (4)$$

$G_{\phi}(\mathbf{r}^{\alpha}, \mathbf{r}'^{\alpha}; N^{\alpha})$ is obtained in the following form

$$G_{\phi}(\mathbf{r}^{\alpha}, \mathbf{r}'^{\alpha}; N^{\alpha}) = \int_{\mathbf{r}^{\alpha}(0)=\mathbf{r}'^{\alpha}}^{\mathbf{r}^{\alpha}(N)=\mathbf{r}^{\alpha}} \mathcal{D}\mathbf{r}^{\alpha}(n) \exp\left(-\frac{3}{2l^2} \int_0^{N^{\alpha}} \left(\frac{d\mathbf{r}^{\alpha}(n)}{dn}\right)^2 dn + i(\beta\tau) \int_0^{N^{\alpha}} \phi(\mathbf{r}^{\alpha}(n)) dn\right) \quad (5)$$

and is clearly nothing but the Green's function of the α th polymeric chain in an external field.²⁷ Because $u(\mathbf{r}, \mathbf{r}')$ is a solution of the Poisson equation we can use its inverse to obtain the following form¹³ for the ϕ average in eq 4

$$\langle \dots \rangle_{\phi} = \int \mathcal{D}\phi(\mathbf{r})(\dots) e^{-\beta\mathcal{H}[\phi]} \quad (6)$$

where $\mathcal{D}\phi(\mathbf{r}) = \lim_{n \rightarrow \infty} d\phi(\mathbf{r}_1) d\phi(\mathbf{r}_2) \dots d\phi(\mathbf{r}_n)$ and

$$\mathcal{H}[\phi] = F_{PB} = -\frac{1}{2} \epsilon \epsilon_0 \int (\nabla\phi)^2 d^3\mathbf{r} - 2kT\zeta \int \cosh(\beta e_0 \phi) d^3\mathbf{r} - \oint \phi \sigma d^2\mathbf{r} \quad (7)$$

is the Poisson-Boltzmann form of the electrostatic free energy of a univalent electrolyte. In eq 6 it has to be evaluated at imaginary values of local potentials or, what amounts to the same thing, at imaginary values of the charges just as in the case of a confined Coulomb fluid.²⁸ We can now take into account all the above developments and derive the final expression for the partition function eq 4 as

$$\Xi = \int \mathcal{D}\phi(\mathbf{r}) e^{-\beta S_{\phi}}, \quad (8)$$

where the action in the exponent can be put into the form

$$S_{\phi} = \mathcal{H}[i\phi] - kT\mathcal{N} \ln\left(\iint G_{\phi}(\mathbf{r}, \mathbf{r}'; N) d^3\mathbf{r} d^3\mathbf{r}'\right), \quad (9)$$

disregarding the possibility of polydispersity of polymeric chains, thus setting $N^{\alpha} = N$ and $G_{\phi}(\mathbf{r}^{\alpha}, \mathbf{r}'^{\alpha}; N^{\alpha}) = G_{\phi}(\mathbf{r}^{\alpha}, \mathbf{r}'^{\alpha}; N)$. A related representation of the partition function in the case of excluded volume interactions is well known.²⁷

The Self-Consistent Field Method

The partition function eq 8 cannot be evaluated analytically. Just as in the case of an electrolyte,²⁹ we thus resort to its approximate evaluation. The self-consistent field (SCF) method provides a good start. The SCF field is obtained as a solution of the saddle-point of the action eq 9

$$\frac{\delta S_{\phi}}{\delta\phi(\mathbf{r})} = 0 \quad (10)$$

We shall not write down this functional derivative explicitly at this stage. To evaluate it, one needs the following identity²⁷ that can be derived from a differential equation corresponding to eq 5, viz.

$$\frac{\delta}{\delta\phi(\mathbf{r})} \ln\left(\iint G_{\phi}(\mathbf{r}, \mathbf{r}'; N) d^3\mathbf{r} d^3\mathbf{r}'\right) = i\beta\tau\rho_{\phi}(\mathbf{r}) = i\beta\tau \frac{\iint d^3\mathbf{r}' d^3\mathbf{r} \int_0^N dn G_{\phi}(\mathbf{r}', \mathbf{r}; N-n) G_{\phi}(\mathbf{r}, \mathbf{r}'; n)}{\iint d^3\mathbf{r} d^3\mathbf{r}' G_{\phi}(\mathbf{r}, \mathbf{r}'; N)} \quad (11)$$

where $\rho_{\phi}(\mathbf{r})$ is the polymer segment density of a single chain at position \mathbf{r} .

The functional derivative eq 10 now decouples into two terms: a volume contribution that amounts to a modified Poisson-Boltzmann equation, and a surface contribution in a form of a

boundary condition, expressing the electroneutrality of the system. It is straightforward to see that the boundary condition demands that the stationary-point ϕ be pure imaginary. Making thus the substitution $\phi \rightarrow i\phi$, one remains with the following saddle-point equations

$$\begin{aligned} \epsilon\epsilon_0\nabla^2\phi(\mathbf{r}) &= 2\zeta e_0\sin h(\beta e_0\phi(\mathbf{r})) - \tau N\rho_\phi(\mathbf{r}) \\ -\epsilon\epsilon_0\frac{\partial\phi}{\partial\mathbf{n}} &= \sigma \end{aligned} \quad (12)$$

where \mathbf{n} is the local normal of the boundary surfaces. Furthermore, the polymer segment density $\rho_\phi(\mathbf{r})$ is obtained via eq 11 from the Green's function eq 5. The definition of the polymer density eq 11 and eq 12 represent the self-consistent field equations for a polyelectrolyte immersed in an electrolyte solution.

The Polyelectrolyte Poisson-Boltzmann Equation

The main conclusions of these rather formal developments can be restated on the basis of purely physical arguments that are standardly used in different derivations of the Poisson-Boltzmann equation.⁷ Because the only mobile charged species in our model system are anions, cations, and charged polymeric chains, the local Poisson equation can be straightforwardly written as

$$\epsilon\epsilon_0\nabla^2\phi(\mathbf{r}) = -\rho(\mathbf{r}) = -\sum_i \rho_i(\mathbf{r}) \quad (13)$$

where $\phi(\mathbf{r})$ is the local mean electrostatic potential at point \mathbf{r} , while $\rho(\mathbf{r})$ is the local total charge density, composed of the local charge density of cations, anions, and polymeric chains (represented by index i). Inserting now all these local charge densities (cationic, anionic, and polymeric) into the Poisson equation, we are led exactly to the first equation of eqs 12, if the polymer density is given by

$$\rho_\phi(\mathbf{r}) = \langle e^{-\beta\tau\phi(\mathbf{r})} \rangle, \quad (14)$$

where now the averaging $\langle \dots \rangle$ has to be done over all the degrees of freedom of the polymer chain. The question now remains of how to represent $\rho_\phi(\mathbf{r})$ explicitly as a function of the local mean potential $\phi(\mathbf{r})$. To do that we assume the ground-state dominance *ansatz*,³⁰ so that the polymer Green's function has the form

$$G_\phi(\mathbf{r}, \mathbf{r}'; N) = G_\phi(z, z'; N) \approx \psi(z)\psi(z')e^{-E_N N} \quad (15)$$

where $|E_N|$ is the lowest lying energy eigenvalue and $\psi(z)$ is the polymer density field. Configurations with negative E_N correspond to the case where polyelectrolyte chain has at least one surface-bound state. With this *ansatz* we are ignoring all effects that depend on the size of the chain.²³ On this level we can eliminate the dependence of the Green's function on the transverse coordinates, thus obtaining $\rho_\phi(z) = (N/S)\psi^2(z)$ with $\int_{-a}^{+a} \psi^2(z) dz = 1$. With these simplifications eqs 12 and the Edwards equation for the Green's function eq 4 are reduced to the following set of two coupled nonlinear equations¹³ for the local average potential $\phi(z)$ and the polymer density field $\psi(z)$

$$\frac{l^2}{6} \frac{d^2\psi}{dz^2} + (E_N - \beta\tau\phi)\psi = 0$$

$$\epsilon\epsilon_0 \frac{d^2\phi}{dz^2} - 2\zeta e_0\sinh(\beta e_0\phi) + \tau N \frac{N}{S} \psi^2 = 0. \quad (16)$$

The impenetrability of the surfaces to polymer beads is now reduced to the boundary condition $\psi(z = \pm a) = 0$, while the appropriate boundary condition for the electrostatic potential can be deduced from eq 12. Equations very similar in content to the above were first derived by Varoqui.³¹

Clearly, in the absence of polymeric chains, the above two equations reduce to the standard Poisson-Boltzmann equation for a uni-uni valent electrolyte. With the polymeric chains present, we can view eqs 16 as a modified Poisson-Boltzmann equation, where the dependence of the polymeric charge density on the mean electrostatic potential has to be determined self-consistently, via the dependence of the polymer density field on the electrostatic potential.

An interesting limit of the above general SCF equations is obtained in the case of a single polyelectrolyte chain³⁴ between two oppositely charged surfaces. In this case, the second equation of the general ground-state dominance SCF equations, eq 16, can be solved analytically leading to a one-dimensional Hartree equation, where the SCF potential is given by $\beta\tau\sigma/\epsilon\epsilon_0 \int_{-a}^{+a} |z - z'|\psi^2(z')dz'$. It is obviously a nonlinear equation, and allows for very complicated behavior including transition between different equilibrium states (see below).

The SCF approach allows also for simple generalizations. Steric interactions between polymer beads¹⁷ can be simply included in the free energy functional as additive terms, and lead to modified SCF equations of a higher order in the polymer density field. Another variation on this set of equations can be obtained if one relaxes the *ansatz* for constrained equilibrium of the polyelectrolyte chains and allows their exchange with the bulk at a fixed chemical potential.¹⁷ This eliminates the Lagrange multiplier for the fixed number of monomers that is, in fact, proportional to E_N . In this case, Borukhov, Andelman, and Orland¹⁷ derive the following set of SCF equations (in our notation)

$$\begin{aligned} \frac{l^2}{6} \frac{d^2\psi}{dz^2} - \beta\tau\phi\psi + v(\psi^3 - \psi_b^2\psi) &= 0 \\ \epsilon\epsilon_0 \frac{d^2\phi}{dz^2} - 2\zeta e_0 \sinh(\beta e_0\phi) \\ + \tau N \frac{N}{S} (\psi^2 - \psi_b^2 e^{-\beta e_0\phi}) &= 0, \quad (17) \end{aligned}$$

where v is the second virial coefficient characterizing steric short-range interactions and ψ_b is the value of the polymer density field in the bulk. This is the most general form of the SCF equations that one can derive.

A linearized form of these SCF equations, that takes into account the short-range steric interactions as well as the equilibrium of the polymers with the bulk, together with an additional chemical surface adsorption term, has been already derived and solved by Joanny.¹⁸

Free Energy, Pressure, and the Contact Theorem

We are now ready to evaluate the surface free energy density defined on the SCF ground-state dominance level by taking into account eqs 16 with the appropriate boundary conditions, and are led to the following explicit form of the surface free energy density

$$\begin{aligned} \mathcal{F} &= -\frac{kT}{S} \ln \Xi = kT N \frac{N}{S} E_N + \frac{F_{PB}}{S} \\ &= kT N \frac{N}{S} \left[\frac{l^2}{6} \int_{-a}^{+a} \left(\frac{d\psi}{dz} \right)^2 dz + \beta\tau \int_{-a}^{+a} \phi \psi^2 dz \right] \end{aligned}$$

$$\begin{aligned} -\frac{1}{2} \epsilon\epsilon_0 \int_{-a}^{+a} \left(\frac{d\phi}{dz} \right)^2 dz - 2kT\zeta \int_{-a}^{+a} \cos h(\beta e_0\phi) dz \\ - 2\phi(z = \pm a)\sigma = \int_{-a}^{+a} f(\psi(z), \phi(z)) dz \quad (18) \end{aligned}$$

where F_{PB} is the standard Poisson-Boltzmann free energy of a nonhomogeneous electrolyte. The local nonequilibrium free energy density f is thus a functional of $\psi(z)$ and $\phi(z)$. This form of the surface free-energy density can be used to derive the SCF equations, eqs 16, which are just its Euler-Lagrange equations. In doing this one should take into account the constrained equilibrium of the chains via a Lagrange multiplier for the constraint $\int_{-a}^{+a} \psi^2(z) dz = 1$. The Lagrange multiplier μ for this constraint turns out to be equal to $kT N(N/S) E_N$.

After deriving the free energy density that leads to correct SCF equations we can now apply the argument of de Gennes,³² together with the first integral of eqs 16 and show that the pressure acting between the two bounding surfaces located at $z = \pm a$ can be reduced to¹³

$$\begin{aligned} \wp &= 2kT\zeta \cosh(\beta e_0\phi(z = a)) \\ &\quad - \frac{1}{2} \frac{\sigma^2}{\epsilon\epsilon_0} + kT N \frac{N}{S} \frac{l^2}{6} \left(\frac{d\psi}{dz} \right)^2_{z=a} \quad (19) \end{aligned}$$

This relation represents an appropriate generalization of the “contact theorem” amply used in the Poisson-Boltzmann theory of interacting double layers to the case with added polyelectrolyte chains. The first two terms of the above equation are clearly identical to the standard Poisson-Boltzmann contact theorem, while the last term embodies the equilibrium of forces due to the presence of polymeric chains.³³

Results

Numerical investigations of the SCF equations can be systematized if one introduces appropriate dimensionless quantities. In the case of polycounterions, no added salt, the solution of eqs 16 appropriately linearized¹³ depends on only one parameter $\lambda_B^{1/3} = (6\beta\tau\sigma/\ell^2\epsilon\epsilon_0)^{1/3}$ of dimension inverse length, characterizing the size of the chain. For small values of the dimensionless quantity $\lambda_B^{1/3}a$, the distribution of the polymer between the surfaces is monomodal (Fig. 3) the lowest energy

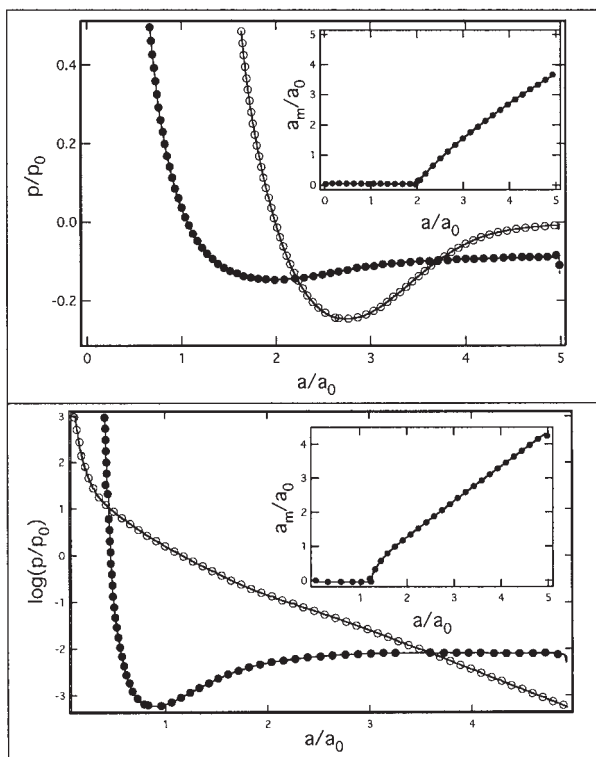


Figure 2. Dimensionless pressure and lowest energy eigenvalue E_N as functions of the dimensionless spacing. The insets show the position of the maxima, a_m of the monomer distribution function as the function of dimensionless coordinate. Upper figure: polycation-only case, filled circles dimensionless pressure, open circles E_N . Lower figure: polyelectrolyte chains with monovalent salt, filled circles log of dimensionless pressure, open circles E_N . For the polycation-only case $a_0 = \lambda_B^{-1/3}$, $p_0 = (\sigma^2/2\epsilon\epsilon_0)$ and for polyelectrolyte plus salt $a_0 = \lambda_D$, $p_0 = (kT/\ell_b\lambda_D^2)$. The values of the parameters (defined in the text) are $\Gamma = 5.4$, $\lambda = 1$ and $\kappa\ell = 1$. Bridging interaction corresponds to negative values of the pressure. Bridging configurations of the chains correspond to bimodal distribution, with $a_m \neq 0$.

eigenvalue varies approximately as a^{-2} , and the pressure is repulsive varying approximately as a^{-3} . At a critical value of the intersurface separation a the polymer distribution becomes bimodal (Fig. 3), and the position of its maximum a_m varies with a , as shown on the inset of Figure 2. At the same time, the pressure turns from repulsion to attraction while the lowest lying energy eigenvalue, E_N , goes through a minimum. At large values of the intersurface separations both the pressure as well E_N decay approximately exponentially and remain attractive.

In the case of polyelectrolyte and salt ions, the main difference in comparison with the previous case is the contribution of the osmotic pressure of the salt ions to the total intersurface pressure.¹³ Here, the solution of the SCF equations, eq 16, depends on four dimensionless parameters: $w_0 = \kappa a$, where κ is the inverse Debye screening length of the salt, dimensionless surface charge $\Gamma = (\beta e_0 \sigma / \epsilon \epsilon_0 \kappa)$, dimensionless electrostatic coupling constant $\lambda = (\beta e_0^2 / \epsilon \epsilon_0 \kappa)(N/S)$, where N is the total number of the polymer beads and S is the surface area of the interfaces and the dimensionless product $\kappa\ell$. These parameters scale the

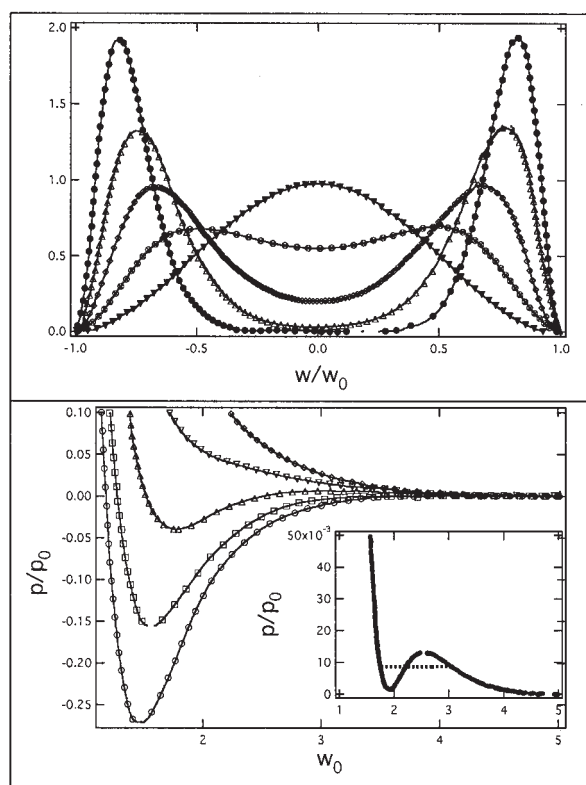


Figure 3. Upper graph, generic form of the monomer density distribution between the charged surfaces. $w_0 = \kappa a$ is the dimensionless separation between the surfaces and $w = \kappa z$ is the dimensionless coordinate in between the surfaces, $-a < z < a$. The graph has been normalized so that w/w_0 is always between 1 and -1 , while for different curves $w_0 = 0.5, 1.5, 2, 2.5, 3$. Lower graph, log of dimensionless pressure for the polyelectrolytes plus univalent salt, same as in Figure 2. $\Gamma = 5.4$ and $\kappa\ell = 1$. Upper curve $\lambda = 0$ and the rest in progressing order $\lambda = 1, 2, 3, 4$. The inset shows the Maxwell construction in the case of pronounced bridging interactions, $\lambda = 2.5$ and $\Gamma = 5.45$, which allows for a coexistence of two phases at different intersurface spacings.

effects of the separation between the surfaces, the charge on the surfaces, the charge on the chains, and the flexibility of the chains. They define different regions in the parameter phase space with different behavior of the interaction pressure.

At small values of $w_0 = \kappa a$ the polymer distribution is monomodal (Fig. 3), with the lowest energy eigenvalue varying approximately as a^{-2} . Again, at a critical value of the intersurface separation the polymer density becomes bimodal (Fig. 3), the lowest lying energy eigenvalue goes through a minimum, but the location of this minimum does not coincide with the monomodal–bimodal transition of the polymer density. This is due to the coupling between the polymer and the salt ion degrees of freedom. The pressure however, has a more complicated behavior due to the presence of the osmotic component of the salt ions. For small enough values of λ it remains purely repulsive over the whole range of a and decays approximately exponentially with a Debye screening length. However, for sufficiently large coupling constants λ , the pressure can also exhibit pronounced attractive regions (Fig. 3). The interplay between attractive polymer-mediated and repulsive osmotic ionic contribution to the total intersurface pressure can lead to phase separation in the system via the Maxwell construction³⁴ (Fig. 3).

In both cases described above, the attractive component of the pressure feeds off the bimodal distribution of the polymer density, which in essence, characterizes bridging configurations: parts of the chain are in close proximity to one of the surfaces and parts to the opposing surface. The intervening part of the chain confers a stretching force that tends to pull the surfaces together. The origin of this stretching force is obviously the connectivity of the chain. The range of this bridging interaction can be seen¹³ to scale as an inverse power of the number of polymer segments, and is thus usually quite small, on the order of the average segment–segment spacing of the polymer, a conclusion consistent also with extensive simulations of the confined polyelectrolyte system³⁵ as well as with other variants of the SCF theory set up specifically for grafted polyelectrolyte chains.³⁶ At very large intersurface spacings, however, there is a residual weak and long ranged pseudo-Casimir attractive interaction stemming from the fluctuations of the local electrostatic field and polymer density field around their respective SCF profiles.³⁷ This weak force would be difficult to detect in simulations, al-

though some indications for its existence can be found in ref. 38.

Generalizing the SCF equations by including also steric effects as well as polymer exchange with the bulk adds additional features to the intersurface interactions. In the low-salt regime a strong repulsion is seen at small separations,¹⁷ followed by a strong attraction due to polyelectrolyte depletion between the surfaces at larger separations. At high-salt concentration the interaction is purely repulsive at all separations and decays exponentially with the Debye screening length. The most interesting results, however, appear to be those where electrostatic and steric interactions as well as chemical equilibrium with the bulk and nonelectrostatic adsorption are treated together on the linearized Debye-Hückel-like level.¹⁸ It was shown that on this level there is a region of the parameter space where the solution of the mean-field equations can give rise to nonmonotonic, oscillatory behavior of the polymer density due to the interplay of the tendency of polyelectrolytes to collapse on macroscopic scales and swell on the microscopic scale due to the presence of counterions. This oscillatory spatial variation of the bulk polymer density persists also for confined adsorbing polyelectrolytes, and in its turn leads to oscillatory polyelectrolyte-mediated interactions. The conclusions of this theory have been completely vindicated by detailed simulation studies that take into account electrostatic as well as steric interactions between polymer segments,³⁹ and appear to be operative also outside the region of the parameter phase space, where the linear theory¹⁸ is supposed to be strictly valid.

POINT MACROIONS—VARIATIONAL THEORY

The Model and Its Hamiltonian

The model system in this case is again quite simple (see Fig. 1); it is composed of two spherical point macroions with M negative fixed charges located at \mathbf{r}_1 and \mathbf{r}_2 , plus two oppositely charged chains, each with N monomers, one positive charge per each monomer, grafted to the macroions. The pair interaction potential $u(\mathbf{r}', \mathbf{r})$ between all the charges in the system will be taken of the screened Coulomb (Debye-Hückel) form²

$$u(\mathbf{r}', \mathbf{r}) = \frac{e^2}{4\pi\epsilon\epsilon_0} \frac{e^{-\kappa|\mathbf{r}-\mathbf{r}'|}}{|\mathbf{r}-\mathbf{r}'|}, \quad (20)$$

κ is the inverse Debye length, e is the charge per each Kuhn's length, and the rest of the notation is standard. Obviously, counterions are not explicitly included in this model, and the difference with the planar case is that from the start we work on the linearized PB (Debye-Hückel) level, and thus this model cannot capture nonlinearities such as charge renormalization or counterion condensation. It can, however, take into account the electrostatic stiffening of the chain⁴⁰ as well as the finite chain size effects.

The interaction potential between the polyelectrolyte chains and the macroion charges is assumed of a similar form viz.

$$\phi_{\text{ext}}(\mathbf{r}) = \frac{e_1 e_0}{4\pi\epsilon\epsilon_0} \frac{e^{-\kappa|\mathbf{r}-\mathbf{r}_1|}}{|\mathbf{r}-\mathbf{r}_1|} + \frac{e_2 e_0}{4\pi\epsilon\epsilon_0} \frac{e^{-\kappa|\mathbf{r}-\mathbf{r}_2|}}{|\mathbf{r}-\mathbf{r}_2|} + \dots, \quad (21)$$

where $\mathbf{r}_1, \mathbf{r}_2$, etc., are the positions of macroions, and their charges are $e_1 = e_2 = Me$, etc. Our model is thus a very straightforward generalization to many macroions of the model used in polyelectrolyte adsorption studies.⁴¹

We will again use the standard continuum model for the polyelectrolyte chain where the mesoscopic Hamiltonian has contributions from chain connectivity, interactions between the segments of the chain, and the interaction with an external field due to the presence of two macroions. It is written as

$$\begin{aligned} \beta\mathcal{H}[\mathbf{r}_i(n)] &= \frac{3}{2\ell^2} \sum_{i=1}^2 \int_0^N \dot{\mathbf{r}}_i^2(n) dn \\ &+ \frac{1}{2} \beta \sum_{i,j=1}^2 \int_0^N \int_0^N u(\mathbf{r}_i(n), \mathbf{r}_j(n)) dn dn' \\ &+ \beta \sum_{i=1}^2 \int_0^N \phi_{\text{ext}}(\mathbf{r}_i(n)) dn, \quad (22) \end{aligned}$$

where $u(\mathbf{r}', \mathbf{r})$ is the pair interaction potential, while $\phi_{\text{ext}}(\mathbf{r})$ is the external interaction potential. The indexes i, j stand for the two polyelectrolyte chains. Clearly, the nonpairwise additive effects such as bridging between multiple macroions mediated by a single chain, have been completely disregarded in this model. The finite macroion size effects have also been disregarded. The grafting of the chains is only taken into account via

their center of mass coordinates in the way explained later.

Variational *ansatz* and Formalism

In what follows now we will closely follow refs. 25 and 42. For the variational *ansatz* corresponding to two chains we will chose a general harmonic hamiltonian of the Feynman-Kleinert form⁴³

$$\begin{aligned} \beta\mathcal{H}_0[\mathbf{r}_i(n)] &= \frac{3}{2\ell^2} \sum_{i=1}^2 \int_0^N \dot{\mathbf{r}}_i^2(n) dn + \frac{3}{2} \sum_{i=1}^2 \zeta_i^2(\mathbf{r}_{0i}) \\ &\times \int_0^N (\mathbf{r}_i(n) - \mathbf{r}_{0i})^2 dn + \beta N \mathcal{L}(\mathbf{r}_{01}, \mathbf{r}_{02}). \quad (23) \end{aligned}$$

This *ansatz* is obviously still dependent on \mathbf{r}_{0i} for $i = 1, 2$, that stand for the centers of mass of the two chains, that is, $\mathbf{r}_{0i} = (1/N) \int_0^N \mathbf{r}_i(n) dn$, as well as the functions $\zeta_i(\mathbf{r}_{0i})$ and $\mathcal{L}(\mathbf{r}_{01}, \mathbf{r}_{02})$ that will be determined variationally. The term with $\zeta_i^2(\mathbf{r}_{0i})$ represents an external harmonic potential, centered on \mathbf{r}_{0i} , that acts either to confine or to expand the chain, depending on its sign. The term $\beta N \mathcal{L}(\mathbf{r}_{01}, \mathbf{r}_{02})$ simply represents the value of this harmonic external potential at the centers of mass of both chains. As will become clear when we proceed, both quantities depend in a complicated way on the interactions between the monomers as well as on the interactions between the monomers and external macroions.

This is not the only possible formulation of the variational approach,⁴⁴ but the results of different formulations are even quantitatively very similar.²⁵

The statistical integral, that is, the partition function for the variational *ansatz* can be obtained in the following form²⁵

$$\begin{aligned} \Xi_0(N) &= \int \mathcal{D}[\mathbf{r}_1(n)] \int \mathcal{D}[\mathbf{r}_2(n)] e^{-\beta\mathcal{H}_0[\mathbf{r}_i(n)]} \\ &= \iint d^3\mathbf{r}_{01} d^3\mathbf{r}_{02} e^{-\beta\mathcal{F}_0(\mathbf{r}_{01}, \mathbf{r}_{02})}. \quad (24) \end{aligned}$$

The two polymer chains are thus represented as two effective Gaussian, Asakura-Oosawa "particles"⁴⁵ with an effective Hamiltonian given by $\mathcal{F}_0(\mathbf{r}_{01}, \mathbf{r}_{02})$. The details of the implementation of the Feynman-Kleinert *ansatz* for (self)interacting

polymer chains have been given before,⁴² and we will rely on the formal developments described in that work. First, we introduce the radius of gyration defined as

$$\begin{aligned} a_i^2(\mathbf{r}_{0i}) &= \frac{1}{3N} \int_0^N \langle (\mathbf{r}_i(n) - \mathbf{r}_{0i})^2 \rangle dn \\ &= \frac{1}{3\zeta_i} \mathcal{L}\left(\frac{\zeta_i \ell^2 N}{2}\right), \end{aligned} \quad (25)$$

where $\mathcal{L}(x) = \cot hx - (1/x)$ is the standard Langevin function. One can then derive⁴² that minimization of the upper bound of the variational free energy with respect to the function $\mathcal{L}(\mathbf{r}_{01}, \mathbf{r}_{02})$ leads to the following equation

$$\begin{aligned} \beta N \mathcal{L}(\mathbf{r}_{01}, \mathbf{r}_{02}) \\ = -\frac{3}{2} \sum_{i=1}^2 \zeta_i^2(\mathbf{r}_{0i}) N a_i^2(\mathbf{r}_{0i}) + \beta W(\mathbf{r}_{01}, \mathbf{r}_{02}). \end{aligned} \quad (26)$$

$W(\mathbf{r}_{01}, \mathbf{r}_{02})$ represents the total interaction free energy, due to self as well as interactions with external fields, of a smeared monomer cloud with a Gaussian density distribution. Let us introduce the combined monomer density function $\rho(\mathbf{r}, \mathbf{r}_{01}, \mathbf{r}_{02})$ and assume it has the form $\rho(\mathbf{r}, \mathbf{r}_{01}, \mathbf{r}_{02}) = \rho_{a_1^2}(\mathbf{r}, \mathbf{r}_{01}) + \rho_{a_2^2}(\mathbf{r}, \mathbf{r}_{02})$, where for each of the chains the monomer density distribution function is given by

$$\rho_{a_i^2}(\mathbf{r}, \mathbf{r}_{0i}) = \frac{N}{(2\pi a_i^2)^{3/2}} \exp -\frac{|\mathbf{r} - \mathbf{r}_{0i}|^2}{2a_i^2}.$$

Then via the self-interaction and interaction with the external fields as in eqs 20 and 21, we obtain

$$\begin{aligned} W(\mathbf{r}_{01}, \mathbf{r}_{02}) &= \sum_{k=1}^2 \mathcal{F}_{a_1^2}(\mathbf{r}_{01} - \mathbf{r}_k) + \sum_{k=1}^2 \mathcal{F}_{a_2^2}(\mathbf{r}_{02} - \mathbf{r}_k) \\ &+ \sum_{k=1}^2 \mathcal{W}_{a_k, a_k}(\mathbf{r}_{0k}, \mathbf{r}_{0k}) + \mathcal{W}_{a_1, a_2}(\mathbf{r}_{01}, \mathbf{r}_{02}). \end{aligned} \quad (27)$$

Here, \mathbf{r}_i stand for the position of the two macroions (to be distinguished from the position of the two centers of mass of the polymer chains \mathbf{r}_{0i}). $\mathcal{F}_{a^2}(\mathbf{r} - \mathbf{r}')$ are due to the interaction of the chains with external fields and can be written in the form

$$\mathcal{F}_{a_i^2}(\mathbf{r} - \mathbf{r}') = \int \frac{d^3 \mathbf{k}}{(2\pi)^3} \rho_{a_i^2}(\mathbf{k}) u(\mathbf{k}) e^{i\mathbf{k}(\mathbf{r} - \mathbf{r}')}. \quad (28)$$

The intra and interchain interactions are given by

$$\mathcal{W}_{a_i, a_j}(\mathbf{r}, \mathbf{r}') = \int \frac{d^3 \mathbf{k}}{(2\pi)^3} \rho_{a_i^2}(\mathbf{k}) u(\mathbf{k}) \rho_{a_j^2}(-\mathbf{k}) e^{i\mathbf{k}(\mathbf{r} - \mathbf{r}')} \quad (29)$$

and represent the electrostatic *self*-energy of the chains and electrostatic interaction energy *between* the chains, where the chains are treated as Gaussian blobs.

Variational Equations

These are straightforward generalizations of the variational theory set up previously for a single chain.⁴² The functions $\zeta_i(\mathbf{r}_{0i})$ are obtained by minimizing the upper bound to the exact free energy with respect to a_i^2 leading to

$$\frac{3}{2} \zeta_i^2(\mathbf{r}_{0i}) N = \beta \frac{\partial}{\partial a_i^2} W(\mathbf{r}_{01}, \mathbf{r}_{02}). \quad (30)$$

The effective centers-of-mass free energy of the two polymer chains is finally given by the expression

$$\begin{aligned} \beta \mathcal{F}_0(\mathbf{r}_{01}, \mathbf{r}_{02}) &= 3 \sum_{i=1}^2 \log \frac{\sinh \frac{\zeta_i \ell N}{2}}{\frac{\zeta_i \ell N}{2}} - \frac{3}{2} \sum_{i=1}^2 \zeta_i^2 N a_i^2 \\ &+ \beta W(\mathbf{r}_{01}, \mathbf{r}_{02}), \end{aligned} \quad (31)$$

The first two terms of this variational free energy represent the entropy of the Gaussian chain, and the last one is due to the interactions with the external fields as well as electrostatic inter- and intrachain interactions (see eq 27). These are the basic equations of the Feynman-Kleinert variational theory as applied to the self interacting polyelectrolyte chains. They are still quite complicated because of the dependence on the center-of-mass coordinates \mathbf{r}_{0i} and the final integration over these variables in eq 24.

If there are no external fields that break the translational symmetry of the problem it can be easily seen⁴² that the dependence on \mathbf{r}_{0i} vanishes, and the solution of the variational equations is

straightforward. With external fields the final quite complicated \mathbf{r}_{0i} integration can be obtained only numerically. In the case that $\mathcal{F}_0(\mathbf{r}_{01}, \mathbf{r}_{02})$ scales with a positive power of N and N is large enough, there is, however, an additional quite accurate approximation to circumvent this final integration.⁴⁶ It consists of the saddle-point evaluation of the final integration with respect to \mathbf{r}_{0i} , that is of an additional minimization of $\mathcal{F}_0(\mathbf{r}_{01}, \mathbf{r}_{02})$ with respect to \mathbf{r}_{01} as well as \mathbf{r}_{02} . If the solutions of these minimization conditions are \mathbf{r}_{01}^* and \mathbf{r}_{02}^* then we obtain from eq 24 a simple explicit and accurate estimate for the free energy of system, viz.

$$\mathcal{F} = -kT\Xi_0(N) \approx \mathcal{F}_0(\mathbf{r}_{01}^*, \mathbf{r}_{02}^*). \quad (32)$$

The solutions of the variational equations have two branches, depending on the relative magnitudes of the interaction with external fields and the self and mutual interaction of the chains. The two branches of the solution are:

1. what we call a *strong coupling branch* that corresponds to $\zeta_i^2(\mathbf{r}_{0i}) > 0$ in the variational equation eq 30, and thus to the dominance of the interactions of the chains with the external macroion fields, the self and mutual interactions of the chains being a small perturbation.
2. and what we term a *weak coupling branch* where $\zeta_i^2(\mathbf{r}_{0i}) < 0$ and thus corresponds to the case where the self and mutual interactions of the chain are dominant, and the interactions with external macroion fields are perturbative. *Coupling* in both cases thus refers to coupling with the external macroion field.

In this model the external macroions break the translational symmetry of the system, and we thus also apply the minimization condition with respect to \mathbf{r}_{01} as well as \mathbf{r}_{02} . To avoid the final complicated integral over the centers of mass of the two polyelectrolyte chains. Taking into account the Gaussian-like form of the function $f_1(y, t)$, we realize that there are, in fact, two different symmetric solutions to this minimization condition: $\mathbf{r}_{01}^* = \mathbf{r}_1$ and $\mathbf{r}_{02}^* = \mathbf{r}_2$, that is, each of the chain remains associated with its grafting macroion and $\mathbf{r}_{01}^* = \mathbf{r}_{02}^* = \frac{1}{2}(\mathbf{r}_1 + \mathbf{r}_2)$, that is, each chain is shared by the two macroions symmetrically. Here we assumed that the first chain is grafted to

the first macroion while the second one is grafted to the second macroion. We refer to the configuration of the polyelectrolyte chains in the first case as *weakly paired* and in the second case as *strongly paired*. The terms are self-explanatory: in the first case, each of the chains is bound to one of the macroions, whereas in the second case they are bound by both of them. In both branches of the solution we can, in general, observe some bridging effects, but they are several orders of magnitude stronger in the first case. Nevertheless, they are always present to some extent.

Solutions of the Variational Equations

As already stated, we consider only symmetric solutions of the variational equations for which $a_1^2 = a_2^2 = a^2$, but in general with $\mathbf{r}_{01}^* \neq \mathbf{r}_{02}^*$. This symmetrization will be applied to results derived below in their final form. We have from the total variational free energy eq 31

$$\beta W(\mathbf{r}_{01}, \mathbf{r}_{02}) = -\frac{\ell_B M N 2^{3/2}}{\pi a} \sum_{i,k=1}^2 f_1\left(\frac{\sqrt{2}}{a} |\mathbf{r}_{0i} - \mathbf{r}_k|, \frac{\kappa a}{\sqrt{2}}\right) + \frac{2\ell_B N^2}{\pi a} f_1(0, \kappa a) + \frac{4\ell_B N^2}{\pi a} f_1\left(\frac{|\mathbf{r}_{01} - \mathbf{r}_{02}|}{a}, \kappa a\right) \quad (33)$$

$$\ell_B = \frac{e_0^2}{4\pi\epsilon\epsilon_0 kT}$$

was introduced above as the Bjerrum length. Also, we introduced the following function

$$f_\lambda(y, t) = \int_0^\infty \frac{u \sin uye^{-\lambda u^2}}{y(u^2 + t^2)} du.$$

On the other hand, the variational equation eq 30 can be obtained just as straightforwardly as,

$$\beta \frac{\partial}{\partial a_1^2} W(\mathbf{r}_{01}, \mathbf{r}_{02}) = \frac{\ell_B N}{\pi a^3} \left[2^{3/2} M \sum_{k=1}^2 g\left(\frac{\sqrt{2}}{a} |\mathbf{r}_{01} - \mathbf{r}_k|, \frac{\kappa a}{\sqrt{2}}\right) - 2Ng\left(\frac{|\mathbf{r}_{01} - \mathbf{r}_{02}|}{a}, \kappa a\right) - Ng(0, \kappa a) \right]. \quad (34)$$

A similar equation could be obtained also for $\beta(\partial/\partial a^2)W(\mathbf{r}_{01}, \mathbf{r}_{02})$ except that \mathbf{r}_{01} on the r.h.s. would be turned into \mathbf{r}_{02} . The following new function was defined above $g(y, t) = -(\partial/\partial \lambda)f_\lambda(y, t)|_{\lambda=1}$. What the variational equation eq 34 really asserts is which terms are important in determining the statistical conformation of the chain, that is, a_i^2 in our case. The first term on the r.h.s. of eq 34 is due to the interactions with the macroions, the second one is due to the interactions between the two chains, and the last one is the self-interaction of the chains. The conformation of the chain as described by a_i^2 is thus determined by the relative magnitudes of these three terms. The final closure for this system of variational equations is provided by the relation between ζ and a , (eq 25).

Strong Coupling Limit, $\zeta^2 > 0$

In this domain of the parameter space the effect of the interactions of the polyelectrolyte chain with the macroions, the term proportional to M in eq 34, determines the overall configuration of the chain. Minimization with respect to $\mathbf{r}_{01}, \mathbf{r}_{02}$ leads first of all to a solution, stable for small values of the separation between the macroions, that corresponds to *strong pairing* configuration of the chain with $\mathbf{r}_{01}^* = \mathbf{r}_{02}^* = \frac{1}{2}(\mathbf{r}_1 + \mathbf{r}_2)$. The variational equation for ζ in this case reads

$$\frac{3}{2} \zeta^2 = \frac{\ell_B N}{\pi a^3} \left[2^{5/2} M g\left(\frac{\sqrt{2}}{2a} |\mathbf{r}_1 - \mathbf{r}_2|, \frac{\kappa a}{\sqrt{2}}\right) - 3Ng(0, \kappa a) \right], \quad (35)$$

while the corresponding free energy has the form

$$\beta \mathcal{F}_0 = 2\beta \mathcal{F}_2(|\mathbf{r}_1 - \mathbf{r}_2|) - \frac{\ell_B N}{\pi a} \times \left(2^{7/2} M \left[f_1\left(\frac{\sqrt{2}}{2a} |\mathbf{r}_1 - \mathbf{r}_2|, \frac{\kappa a}{\sqrt{2}}\right) \right] - 6Nf_1(0, \kappa a) \right). \quad (36)$$

The form of the dependence $\mathcal{F}_2(|\mathbf{r}_1 - \mathbf{r}_2|)$ is, of course, given implicitly via the dependence of ζ and a . Once again, the chain here is bound to both macroions, and its statistical properties are dominated mostly by the interaction with the charges on the macroions. One would expect that the polyelectrolyte mediated interactions between the macroions would be strongest in this case. Obvi-

ously, for large enough $|\mathbf{r}_1 - \mathbf{r}_2|$ the r.h.s. of eq 35 can become negative, going first through zero. This is due to the fact that $g(y, t)$ is a decaying function of y . At this point the above solution ceases to be stable and we have a transition from the *strongly paired* to *weakly paired* branch of the strong coupling limit. The transition depends on the macroion parameters such as the magnitude of their charges as well as the length of the chains. In this sense, it represents a finite size (of the chains) effect.

The *weakly paired* configuration is characterized by $\mathbf{r}_{01}^* = \mathbf{r}_1$ and $\mathbf{r}_{02}^* = \mathbf{r}_2$, and is the stable branch at larger separations between the macroions. Here, the variational equation for ζ becomes

$$\frac{3}{2} \zeta^2 = \frac{\ell_B N}{\pi a^3} \left[2^{3/2} M \left[g\left(0, \frac{\kappa a}{\sqrt{2}}\right) + g\left(\frac{\sqrt{2}}{a} |\mathbf{r}_1 - \mathbf{r}_2|, \frac{\kappa a}{\sqrt{2}}\right) \right] - 2Ng\left(\frac{|\mathbf{r}_1 - \mathbf{r}_2|}{a}, \kappa a\right) - Ng(0, \kappa a) \right], \quad (37)$$

The corresponding free energy in this case can be obtained as

$$\beta \mathcal{F}_0 = \beta \mathcal{F}_2(|\mathbf{r}_1 - \mathbf{r}_2|) - \frac{\ell_B N}{\pi a} \left(2^{5/2} M \left[f_1\left(0, \frac{\kappa a}{\sqrt{2}}\right) + f_1\left(\frac{\sqrt{2}}{a} |\mathbf{r}_1 - \mathbf{r}_2|, \frac{\kappa a}{\sqrt{2}}\right) \right] - 4Nf_1\left(\frac{|\mathbf{r}_1 - \mathbf{r}_2|}{a}, \kappa a\right) - 2Nf_1(0, \kappa a) \right). \quad (38)$$

The most important term to determine the conformation of the chain is the interaction with the single macroion, and is thus only weakly dependent on the separation between them. These are the first and the last term in the r.h.s. of eq 38. The separation-dependent terms act only as a perturbation to these terms. It is thus to be expected that the polyelectrolyte mediated interactions will be much weaker in this case.

Weak Coupling Limit, $\zeta^2 < 0$

In this case, the effect of electrostatic self-interaction is dominant, and would lead to stiffening up the chain, giving it a rod-like appearance quantified by the scaling $a \sim N$. We expect that even with external fields originating at the

macroions the chain will essentially assume this type of extended configurations in this limit, modified only perturbatively by the effect of both macroions. Simulations of single chain adsorption⁴¹ are completely consistent with this picture because for large N protruding rod-like tails are observed that correspond to electrostatically stiffened portions of the chain. Calculations of Nguyen and Shklovskii⁴⁷ also lead to the same qualitative picture of chain adsorption in this limit. Because in this limit the effect of the macroions is small, the polyelectrolyte chains can never be *strongly paired* by both macroions. We thus remain solely with the *weakly paired* configuration of the chains due to the grafting to the macroions. The solution of the variational equation eq 30 thus only has one branch in this case given by

$$\frac{3}{2} \zeta^2 = \frac{\ell_B N}{\pi a^3} \left[2Ng \left(\frac{|\mathbf{r}_1 - \mathbf{r}_2|}{a}, \kappa a \right) + Ng(0, \kappa a) - 2^{3/2} M \left[g \left(0, \frac{\kappa a}{\sqrt{2}} \right) + g \left(\frac{\sqrt{2}}{a} |\mathbf{r}_1 - \mathbf{r}_2|, \frac{\kappa a}{\sqrt{2}} \right) \right] \right], \quad (39)$$

Clearly, this equation is obtained by the substitution $\zeta \rightarrow i\zeta$ from eq 30. This transformation should be taken into account also in eq 25 leading to

$$\alpha^2 = \frac{1}{3\zeta} \mathcal{L}' \left(\frac{\zeta \ell^2 N}{2\sqrt{3}} \right),$$

where now $\mathcal{L}'(x) = (1/x) - \cot x$. The interaction with the macroion, the M term in the eq 39, can modify the value of the size of the chain, but it has no effect any more on the stability of the solution.

The corresponding free energy is given by an equation similar to eq 38 but with the change $\zeta \rightarrow i\zeta$ well taken into account in $\mathcal{F}_2(|\mathbf{r}_1 - \mathbf{r}_2|)$. It leads to the following result

$$\beta \bar{\mathcal{F}}_0 = 6 \log \frac{\sin \frac{\zeta \ell N}{2}}{\frac{\zeta \ell N}{2}} + 3\zeta^2 N a^2 - \frac{\ell_B N}{\pi a} \left(2^{5/2} M \left[f_1 \left(0, \frac{\kappa a}{\sqrt{2}} \right) + f_1 \left(\frac{\sqrt{2}}{a} |\mathbf{r}_1 - \mathbf{r}_2|, \frac{\kappa a}{\sqrt{2}} \right) \right] - 4Nf_1 \left(\frac{|\mathbf{r}_1 - \mathbf{r}_2|}{a}, \kappa a \right) - 2Nf_1(0, \kappa a) \right). \quad (40)$$

Again, because the solution of the variational equations here remains on a single branch all the time, showing no jump from one stable branch to another one (“snapping” of the chain, see below). The free energy shows no discontinuities either, although it still depends on the separation between macroions.

Results

Qualitative features of the numerical solutions of the variational equations, the details of which are discussed in ref. 25, can be systematized by analyzing first the strong and then the weak coupling limit for two substantially different values of the Debye length, that is, salt activity. In the strong coupling limit the free energy and the size of the chain are given on Figure 4 for ionic strengths 1 mM and 60 mM, as functions of the separation between the macroions. At small separation the free energy is dominated by the bare screened Coulomb repulsion. The chains are in the strongly paired configuration, thus adsorbed to *both* macroions symmetrically, and their size in general follows the increase in the separation between the macroions. This stretching of the chains gives rise to an attractive contribution to the interaction free energy that becomes dominant for intermediate macroion separations, giving rise to strong bridging interactions. The bridging interactions are composed of configurational part as well as electrostatic parts.

Increasing the separation further starts to change the balance of the two terms in eq 35. At a crossover separation between the macroions, $|\mathbf{r}_1 - \mathbf{r}_2| = D_c$, when $\zeta^2 = 0$, corresponding to

$$2^{5/2} M g \left(\frac{\sqrt{2}}{2a} D_c, \frac{\kappa a}{\sqrt{2}} \right) = 3Ng(0, \kappa a) \quad (41)$$

there is an instability point and the chains snap from strongly to weakly paired configuration, thus from being adsorbed to both macroions symmetrically to being adsorbed each to its own grafting macroion. The crossover separation given by the solution of eq 41, obviously depends on M , N and κa .

This snapping is seen as a clear break in the dependence of the size of the chain on the macroion separation, and is observed also in simulation.¹⁶ The snapping of the chains from strongly to weakly paired configuration is not due to their grafting to the macroions but rather to the intri-

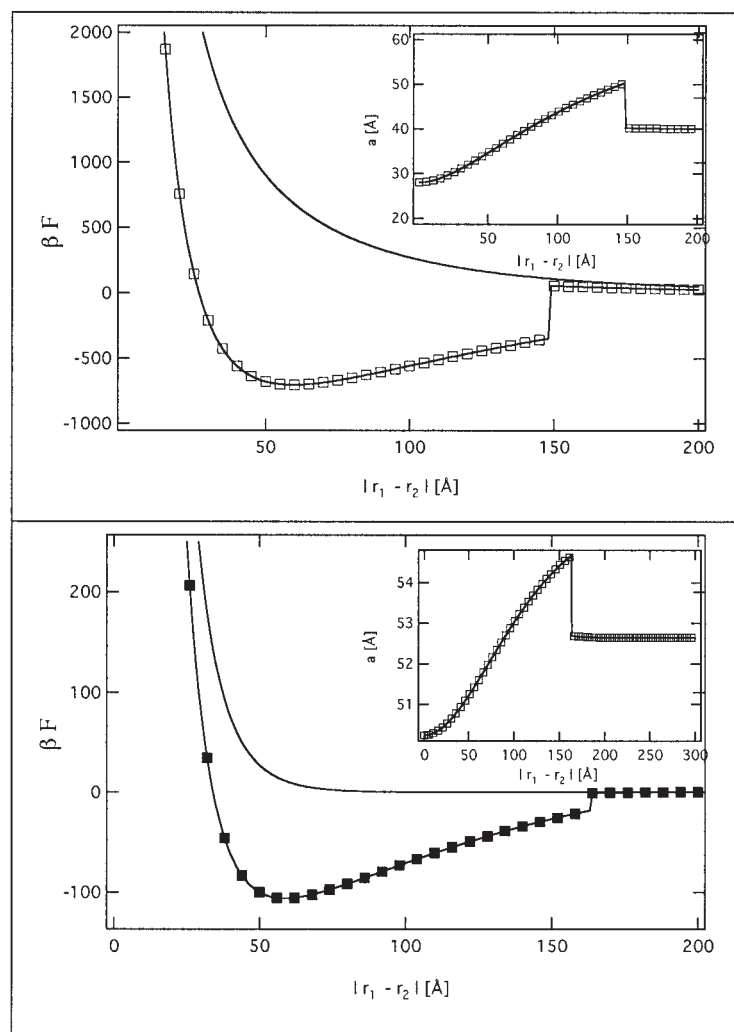


Figure 4. Macroion interaction free energy eq 36 as a function of separation between the macroions $|\mathbf{r}_1 - \mathbf{r}_2|$ in the strong coupling limit. $M = 100$ and $N = 30$ in 1 mM (upper curve) and 60 mM (lower curve) univalent electrolyte. The insets show the radius of gyration eq 25 of the chain. For comparison, the bold line represents the screened Coulomb interactions between two bodies each bearing M elementary charges. The region of separations with attractive polyelectrolyte-mediated interactions coincides with the bridging region of polyelectrolyte conformations, see inset.

cate interplay between the entropy and the energy of the chain configurations. After the two chains snap from the bridging configuration they remain centered each on its own grafting macroion, renormalizing its effective charge. The bridging contribution to the interaction free energy disappears and the remaining interaction is again screened Coulomb with a renormalized value of the effective charge on the macroion. The qualitative picture of polyelectrolyte-mediated interaction provided by the variational approach is completely consistent with existing simulation data

for one chain¹⁶ or several chains⁴⁸ in the field of two macroions. The snapping of the chain at intermediate spacing appears to be a salient feature of the configurations of the chain in the strong coupling limit, and is a consequence of the interplay between the energy and the entropy of the chain configurations.

The effect of the salt in the strong coupling regime can be simply understood via screening of the interactions between the polyelectrolyte chains and the macroions. For large salt activity the bridging contribution becomes quenched and

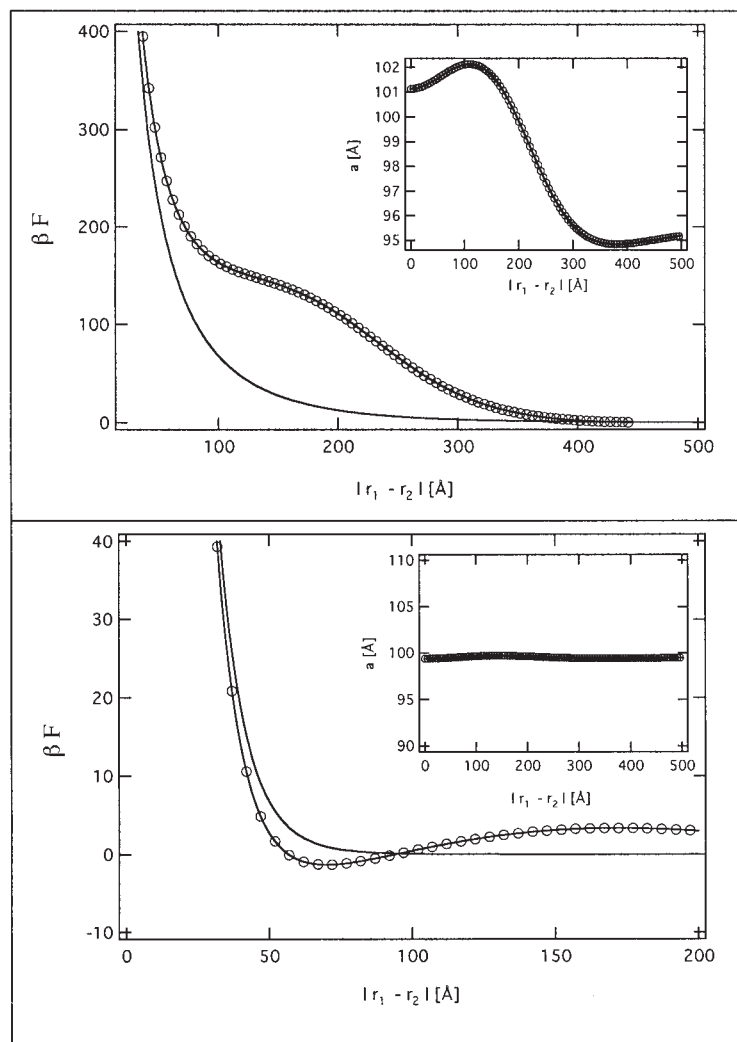


Figure 5. Macroion interaction free energy eq 40 in the weak coupling limit. $M = 40$ and $N = 50$ in 1 mM (upper curve) and 60 mM (lower curve) univalent electrolyte. The insets show the radius of gyration of the chain. Again, for comparison, the bold line represents the screened Coulomb interactions between two bodies each bearing M elementary charges. The bridging configurations of the chains are missing now, and the bridging interaction itself is extremely attenuated (note the scale of the free energy). The enhanced repulsion is due to “coronal” interpenetration of the extended chains.

would eventually disappear altogether. Also, the variation of the size of the chain with the separation between the macroions becomes less pronounced for larger screening.

Contrary to this case, in the weak coupling limit there is a clearly discernible (see Fig. 5), *repulsion* at smaller separations. It is due to the interpenetrating “coronas,” that is, extended configurations of the grafted chains, on approach of the macroions. These extended conformations of the chain have been clearly seen also in simulations⁴¹ and are due to electrostatic stiffening of

the chain; in other words, they are due to the electrostatic self-interactions of the chains. Should we have many chains grafted to both macroions instead of just two, this incipient repulsion would develop into a full-blown brush repulsion regime.¹¹ Because we have only one chain per macroion the effect of “coronal” interpenetration is rather weak, but nevertheless clearly discernible. Its range depends on the size of the chain N as well as the amount of salt that regulates the overall extension of the chain and quenches the “coronal” repulsion.

In the weak coupling limit the chain conformations are always in the weakly paired configuration, and there is no snapping of the chain. The residual bridging attraction is very weakened (note the energy scale on Fig. 5), and is in constant competition with repulsive “coronal” interpenetration interactions. The effect of the separation between the macroions on the size of the chains is opposite to the one observed in the strong coupling limit. The extent of the chain is thus largest at smaller separations where the “coronal” interpenetration forces the chains to extend into space.

OUTLOOK

Bridging interactions in both contexts, interactions between charged planar, as well as charged point macroions, are thus a consequence of the polyelectrolyte chain configurations driven by the electrostatic interactions with external fields. Because the charge on the macroions is of the opposite sign from the charge on the polyelectrolyte, the chains are invariably attracted to the macroions while the parts of the chain spanning the region between the macroions act as bridges. The entropic and energetic cost of these bridges gives rise to an attractive contribution to the interaction free energy, that is, to bridging interactions. The rest is details, and there are many.

The theoretical framework in which we formulated the description of the bridging effects is, in many respects, quite restrictive. First of all, we completely disregarded all electrostatic correlation effects that cannot be formulated in the framework of the SCF or the Debye-Hückel variational theory. These effects, which have not been properly addressed in the bridging context, become dominant for higher valency counterions, and can lead to a reversal of sign of the electrostatic interactions.⁴⁹ Correlation effects of polymer configurations have also been shown to lead to an effective weak long-range pseudo-Casimir tail in the bridging attraction.³⁷

The nature of the SCF approximation in the planar case also does not allow us to include the effects of electrostatic stiffening of the chain⁴⁰ into the formalism. Contrary to this case, for point macroions the variational approach can describe the electrostatic stiffening of the chain on the Odijk-Skolnick-Fixman level.⁵⁰ This effect is

also driving the separation dependence of the polymer-mediated interaction in the weak coupling limit as described above. For the planar case with grafting also taken into account it should lead to more brush-like behavior of the interaction.

The ground-state dominance *ansatz* in the planar case does not allow us to address the finite size effects, although this shortcoming could be easily implemented if higher eigenvalues would be taken into account.²³ More serious drawbacks are due to the fact that we ignored the grafting of the chains to the surfaces. Again, for small grafting densities this would not make a whole lot of difference, but for higher grafting density the system would start to exhibit the behavior of interacting polyelectrolyte brushes, which is very much different from the bridging regime.¹¹

The approximation of fixed charges on the polyelectrolyte can also be made more realistic by assuming either a quenched or annealed distribution along the chain. Annealed distribution of charges in general makes the free energy smaller, and would thus lead to stronger attraction or more pronounced bridging contribution.⁵¹

The main drawback of the variational formulation of the bridging interaction in the case of small macroions is the linearized (Debye-Hückel) form of electrostatics. All nonlinear effects are thus *a priori* excluded. On this level, the main effect of the salt is to attenuate the bridging interaction as well as the repulsive interaction between the polyelectrolyte “coronas.” In this respect the variational approach is inferior to the ground-state dominance *ansatz*. One possible way out would be to formulate also the electrostatic part of the problem on a variational level,⁵² where all the Debye-Hückel parameters would be determined self-consistently.

Another important omission of the variational approach is the size of the macroions. The finite size of the chain in weakly paired or strongly paired configuration clearly showed by the numerical results is thus not due to the finite size of the adsorbing macroions as in more realistic simulations,⁴¹ but is an entropy-energy competition effect: high adsorption energy versus low configurational entropy in the weakly paired state, leading to the finite size of the weakly paired state even with a point adsorbing macroion. This type of finite size effect can be straightforwardly incorporated into the statistics of free, noninteracting chains,⁵³ but would be difficult to incorpo-

rate into the Feynman-Kleinert variational method, and were thus ignored in our formulation. Alternative approaches would thus have to be considered.⁵⁴

Although bridging effects are well documented in different contexts of the colloid science, it remains to be seen just what is their role in biological milieu. Recent experiments on the second virial coefficient of the nucleosomal core particles⁵⁵ can be interpreted at least in part as a bridging effect. Nevertheless, further work is necessary to understand the detailed properties of polyelectrolyte bridging in more complex biological environments.

I would like to acknowledge illuminating discussions with David Andelman, Roland Netz, Oleg Borisov, Theo Odijk, Luc Belloni, Per Lyngs Hansen, and Adrian Parsegian. I am especially grateful to Andrei Brukhno for his careful reading of the MS and for his many suggestions and comments that greatly improved the article. Parts of the present research were performed with the help of Chercheur Associe fellowship of C.N.R.S., which is gratefully acknowledged.

REFERENCES

- Oosawa, F. *Polyelectrolytes*; Dekker: New York, 1971.
- Barrat, J.-L.; Joanny, J.-F. *Adv Chem Phys* 1996, 94, 1.
- Rubinshtein, M.; Colby, R. H. *Polymer Physics*; Oxford University Press: Oxford, 2003.
- Napper, D. *Polymeric Stabilisation of Colloidal Dispersions*; Academic Press: New York, 1983.
- Boal, D. *Mechanics of the Cell*; Cambridge University Press: Cambridge, 2002.
- For a good introduction see: Holm, C.; Kekicheff, P.; Podgornik, R., Editors; *Electrostatic Effects in Soft Matter and Biophysics*; Kluwer Academic Publishers: New York, 2001.
- Derjaguin, B. V.; Churaev, N. V.; Muller, V. M. *Surface Forces*; Consultants Bureau: New York, 1987.
- Evans, D. F.; Wennerström, H. *The Colloidal Domain: Where Physics, Chemistry, Biology, and Technology Meet*; John Wiley and Sons: New York, 1999.
- Verwey, E. J. W.; Overbeek, J. Th. G. *Theory of the Stability of Lyophobic Colloids*; Dover: New York, 2000.
- Mahanty, J.; Ninham, B. W. *Dispersion Forces*; Academic Press: New York, 1976.
- Netz, R. R.; Andelman, D. *Phys Rep* 2003, 380, 1–95.
- Luckham, P. F.; Klein, J. *J Chem Soc Faraday Trans 1* 1984, 80, 865; Claesson, P. M.; Ninham, B. W. *Langmuir* 1992, 8, 1406–1412; Dahlgren, M. A. G. *Langmuir* 1994, 10, 1580; Lowack, K.; Helm, C. A. *Macromolecules* 1998, 31, 823; Abraham, T.; Kumpulainen, A.; Xu, Z.; Rutland, M.; Claesson, P. M.; Masliyah, J. *Langmuir* 2001, 17, 8321.
- Podgornik, R. *J Phys Chem* 1991, 95, 5249; Podgornik, R. *J Phys Chem* 1992, 96, 884.
- Åkesson, T.; Woodward, C.; Jönsson, B. *J Chem Phys* 1989, 91, 2461.
- Böhmer, M. R.; Everaers, O. A.; Scheutjens, J. M. H. M. *Macromolecules* 1990, 23, 2288.
- Podgornik, R.; Jönsson, B. *Europhys Lett* 1993, 24, 501; Podgornik, R.; Åkesson, T.; Jönsson, B. *J Chem Phys* 1995, 102, 9423.
- Borukhov, I.; Andelman, D.; Orland, H. *J Phys Chem* 1999, 103, 5042.
- Châtellier, X.; Joanny, J.-F. *J Phys II (France)* 1996, 6, 1669.
- Richmond, P. *J Phys A* 1973, 6, L109.
- de Gennes, P.-G.; Pincus, P.; Velasco, R. M.; Brochard, F. *J Phys (France)* 1976, 37, 1461.
- Eisenriegler, E. *Polymers Near Surfaces: Conformation Properties and Relation to Critical Phenomena*; World Scientific Pub Co: Singapore, 1993; Cohen Stuart, M. A.; Fleer, G. J.; Scheutjens, J. M. H. M.; Cohen Stuart, M. A. *Polymers at Interfaces*; Chapman and Hall: London, 1993.
- Muthukumar, M. *J Chem Phys* 1987, 86, 7230.
- van Opheusden, J. H. J. *J Phys A Math Gen* 1988, 21, 2739.
- Israëls, R.; Scheutjens, J. M. H. M. (unpublished) 1990.
- Podgornik, R. *J Chem Phys* 2003, 118, 11286.
- Borukhov, I.; Andelman, D.; Orland, H. *Eur Phys J* 1998, 5, 869.
- Doi, M.; Edwards, S. F. *The Theory of Polymer Dynamics* 1986; Clarendon Press: Oxford, 1986.
- Podgornik, R.; Žekš, B. *J Chem Soc Faraday Trans 2* 1988, 84, 611; Netz, R. R.; Orland, H. *Europhys Lett* 1999, 45, 726.
- Netz, R. R. *Eur Phys J E* 2001, 5, 557.
- de Gennes, P.-G. *Scaling Concepts in Polymer Physics*; Cornell University Press: Ithaca, NY, 1979.
- Varoqui, R. *J de Physique II* 1993, 3, 1097.
- de Gennes, P.-G. *Macromol* 1982, 15, 492.
- Podgornik, R. *J Phys Chem* 1993, 97, 3927.
- Podgornik, R. *Croat Chem Acta* 1992, 65, 285.
- Dahlgren, M.; Waltermo, A.; Blomberg, E.; Claesson, P. M.; Sjöström, L.; Åkesson, T.; Jönsson, B. *J Phys Chem* 1993, 97, 11769.
- Miklavcic, S. J.; Woodward, C. E.; Jönsson, B.; Åkesson, T. *Macromolecules* 1990, 23, 4149.
- Podgornik, R.; Dobnikar, J. *J Chem Phys* 2001, 115, 1951.

38. L. Sjostrom, Ph.D. Thesis, University of Lund, 1998.
39. Jönsson, B.; Broukhno, A.; Forsman, J.; Åkesson, T. (preprint) 2003.
40. Ullner, M. *J Phys Chem B* 2003, 107, 8097.
41. Chodanowski, P.; Stoll, S. *Macromol* 2001, 34, 2320.
42. Podgornik, R. *J Chem Phys* 1993, 99, 7221.
43. Feynman, R. P.; Kleinert, H. *Phys Rev A* 1986, 34, 5080.
44. Gurovitch, E.; Sens, P. *Phys Rev Lett* 1999, 82, 339; Golestanian, R. *Phys Rev Lett* 1999, 83, 2473.
45. Asakura, S.; Oosawa, F. *J Polym Sci* 1958, 33, 183.
46. Büttner, H.; Flytzanis, N. *Phys Rev A* 1987, 36, 3443.
47. Nguyen, T. T.; Shklovskii, B. I. *Physica A* 2001, 293, 324.
48. Dzubiella, J.; Moreira, A. G.; Pincus, P. A. *Macromol* 2003, 36, 1741.
49. Netz, R. R. *Eur Phys J E* 2001, 5, 557.
50. Podgornik, R.; Hansen, P. L.; Parsegian, V. A. *J Chem Phys* 1999, 113, 9343.
51. Borukhov, I.; Andelman, D.; Orland, H. *Europhys Lett* 1995, 32, 499.
52. Diehl, A.; Barbosa, M. C.; Levin, Y. *Phys Rev E* 1997, 56, 619.
53. Birshtein, T. M.; Borisov, O. V. *Polymer* 1991, 32, 916.
54. Boroudjerdi, H.; Netz, R. R. *Europhys Lett*, 2003, 64, 413.
55. Mangenot, S.; Raspaud, E.; Tribet, C.; Belloni, L.; Livolant, F. *Eur Phys J E* 2002, 7, 221.